Indian Journal of Pure & Applied Physics
Vol. 63, February 2025, pp. 152-160
DOI: 10.56042/ijpap.v63i2.15108

Compact High Gain and Bandwidth Enhanced RFID Reader Antenna for Handheld Applications

Abhishek Choudhary & Deepak Sood

Department of Electronics and Communication Engineering, University Institute of Engineering and Technology, Kurukshetra University, Kurukshetra136119, India

Received 15 November 2024; accepted 27 January 2025

A compact UHF RFID reader antenna, designed for handheld applications, has been proposed to meet the requirements for high gain and wide bandwidth. The designed antenna exhibits linear polarization and delivers a maximum gain of 6.46 dBi along with a radiation efficiency of more than 90%. Furthermore, it achieves a maximum front-to-back ratio (FBR) of 19.75 dB and a 10 dB impedance bandwidth of 13.77 % spanning 125 MHz (from 845 to 970 MHz), thus covering the entire UHF RFID band (860 – 960) MHz making it suitable for various real-world applications such as in logistics, inventory management, asset tracking, healthcare and supply chain management. Notably, the antenna's compact profile, measuring (100×100×1.6) mm³ or equivalently 0.3λ×0.3λ×0.004λ relative to the center frequency of the operational band (907 MHz), facilitates seamless integration within handheld readers. A prototype of the design is fabricated on an FR4 substrate and its performance is experimentally verified.

Keywords: Reader antenna; RFID (Radio Frequency Identification); Yagi Uda; UHF (Ultra High Frequency); Wideband

1 Introduction

The RFID system is a rapidly growing technology that uses RF signals for the automatic identification of objects. RFID technology is being exploited for many applications such as agriculture, healthcare, libraries, airports, military, passports, supply chains, mobile payments, *etc*.[1]. In terms of the operating frequencies, each country has its own allocation at UHF band i.e. 866-869MHz in Europe, 866-867MHz in India, 902-928 in America, and in Japan as reported[2].

In recent years, there has been a significant transition within the domain of radio frequency identification (RFID) systems, shifting from stationary RFID setups to the adoption of mobile RFID technology. This evolution is primarily motivated by the enhanced convenience offered by mobile RFID, wherein it often proves more practical to move a reader antenna towards the target object rather than vice versa. This progression foresees the emergence of reader antennas tailored for handheld applications, necessitating specific design considerations. Therefore, handheld reader antennas are distinguished by their compact dimensions, long-range capabilities, lightweight construction, high-gain attributes aimed a text ending battery life, and a favorable front-to-back (F/B) ratio designed to minimize electromagnetic (EM) energy absorption. Various methodologies have been explored to achieve these desired characteristics. The utilization of reflecting surfaces[3-7] enhances the performance of the reader antenna by improving the impedance matching, directivity, and radiation efficiency. In such designs, the precise alignment with the antenna structure and the potential for unwanted reflections causing signal distortion present significant challenges for achieving optimal performance. Furthermore, the incorporation of superstrate materials[8] introduces manufacturing complexity and increases the overall size and thickness of the antenna, thereby limiting its potential applications. Further, the electromagnetic band gap (EBG) structures are typically engineered to suppress specific frequency bands, resulting in narrowband operation for RFID reader antennas[9]. Additionally, slot configurations[10-11] exhibit large bandwidths, but lower gain potentially limits the antenna's versatility across a broad range of frequencies.

To design a RFID reader antenna, the strategic placement of elements in array configurations[12-14] can improve the read range and exhibit wide coverage. The log-periodic dipole array, reported in[12], promises high gain and wideband attributes but requires the use

Corresponding author:(E-mail:choudhary.abhi16@gmail.com)

of extra parasitic strips for enhancement of front-to-back ratio, thereby increasing the size and require rigorous optimization. High-gain Yagi-Uda arrays in[13-14] are constrained by a narrow 80 MHz bandwidth, restricting their applicability in universal RFID contexts. Therefore, careful evaluation and planned selection of antenna design techniques are important to achieve an optimal balance between performance, size, and complexity in handheld RFID systems. Further, circularly polarized antenna configurations have been reported to design reader antennas[5, 15]. These antennas are designed using L-inverted strips and inverted F strips, respectively and both are fed using a power divider whose ports are matched using chip resistors to achieve circular polarization. Circularly polarized antennas are basic for ensuring the efficient reading of RFID tags, irrespective of their orientation in relation to the reader antenna. However, interaction of a linearly polarized RFID tag with circularly polarized reader antenna, results a diminished received power compared to linearly polarized counterparts. This decrease in power reception arises from the power division across two planes inherent to circular polarization[16].Consequently, the compromised power reception may obstruct the tag's responsiveness to the reader's signals, potentially reducing the read range. To overcome this challenge, linearly polarized reader antennas emerge as a preferable choice for handheld reader devices. The manual rotation capability of these antennas facilitates efficient tag orientation management while ensuring a longer read range. Alternative designs, such as helical antennas detailed in[17-18], offer directional accuracy, gain, and frequency adaptability. Nonetheless, their bulkiness poses limitations for handheld use, constituted by narrow bandwidth challenges. Planar configurations discussed in references[19,20] present compact solutions, but with bandwidth constraints in [19] and low gain in[20]. Edge-fed reader antennas, as described in[21-22], generate surface waves and undesired cross-polarization radiations. Dipole based antenna design, reported in[23], exhibit omnidirectional coverage but deals with trade-offs in gain and bandwidth. Meandering techniques proposed in [24] yield compact, high-gain reader antennas but at the expense of limited bandwidth. Similarly, equilateral triangular monopole antennas in[25] exhibit wide-band operation but suffer from low gain. Yagi-Udaarray-based designs detailed in[26-27]exhibit wide band width but with moderate gain.

Hence, to overcome the aforementioned problems and to achieve high gain, a good front-to-back ratio, compactness, and lightweight design, the Yagi-Uda structure is chosen. This structure can be utilized to obtain wideband/multiband functionality by incorporating different methods, such as exciting the antenna with a microstrip feed line in multi-mode operations[28-29], placing the antenna in close proximity to an EBG ground plane[30], incorporating a pair of strip lines with capacitors[31], or integrating multi-branch elements[32]. Pattern reconfiguration and multi-input multi-output (MIMO) functionality can also be achieved, as discussed in[33-35]. However, these techniques increase design and fabrication complexity. Furthermore, antenna designs using these methods tend to increase the overall size of the antenna for the UHF RFID band. Therefore, in this paper, a simple-to-fabricate, compact, lightweight Yagi-Uda structure is proposed, which provides wide bandwidth, high gain, and a good front-to-back ratio in the UHF RFID band. With slight optimization of the dimensions of the three elements, full coverage of the UHF band with high gain is achieved. The proposed antenna provides a bandwidth of 125 MHz, from 845 MHz to 970 MHz, which covers the entire UHF RFID band (860-960 MHz) as regulated by ISO 18000-6C.

2 Design and Simulation

The configuration of the proposed RFID reader antenna is shown in Fig. 1. The design consists of three elements that are reflector, driven element and director.

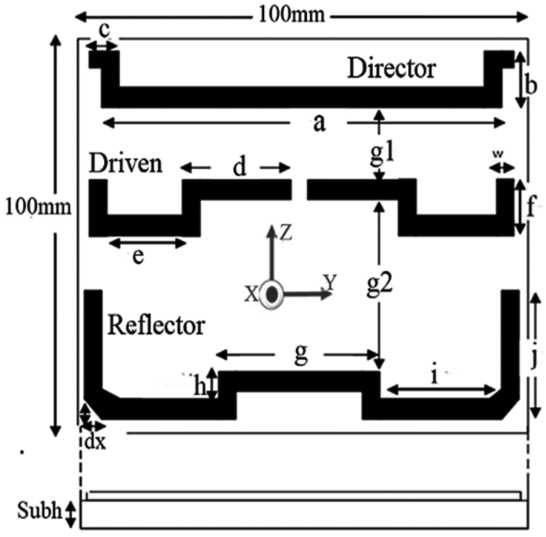

Fig. 1 — The design configuration of the proposed Yagi-Uda antenna

The top layer pattern is printed on a copper-coated 1.6 mm thick and (100×100) mm^2 FR4 substrate (ε_r = 4.4, tanδ = 0.02). The thickness of the copper layer is 26 μm. The antenna is fed through a coaxial feed connected with a driven element. The lengths of elements are slightly meandered to reduce the size of the antenna and to achieve the desired characteristics. The proposed antenna has a compact size of 0.3λ × 0.3λ × 0.004λ at the center frequency of 907 MHz, enabling its use in handheld RFID readers where size constraints are paramount. The optimized dimensional parameters of the antenna are listed in Table.1

2.1 Antenna Design process

The design process is initiated by designing a half wave meandered dipole antenna on an un-grounded FR4 substrate of thickness 1.56 mm as shown in Fig. 2(a). The meandering is done to reduce the size of the antenna. This half wave driven element (Antenna 1) exhibits resonance at 910 MHz. In order to get better physical insight of the design, the impedance and radiation characteristics are studied for UHF RFID band as shown in Fig. 3. It is

Table 1 — Dimensional Parameters of antenna

Parameters	Dimensions (mm)	Parameters	Dimensions (mm)
a	93	G	44
b	15	H	9
c	3	I	24
d	32	J	24
e	14	dx	3
f	13.5	g1	19
w	2	g2	51

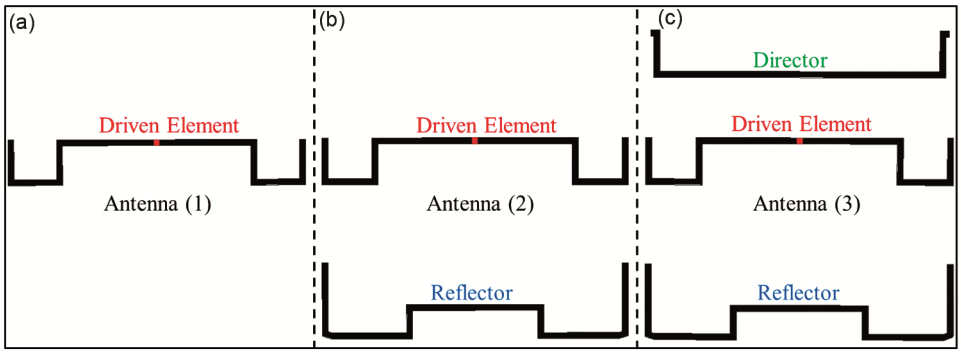

Fig. 2 — Design Process of the proposed antenna. (a) Meandered driven element, (b) meandered driven element and parasitic reflector, and (c) meander driven element with parasitic reflector and director

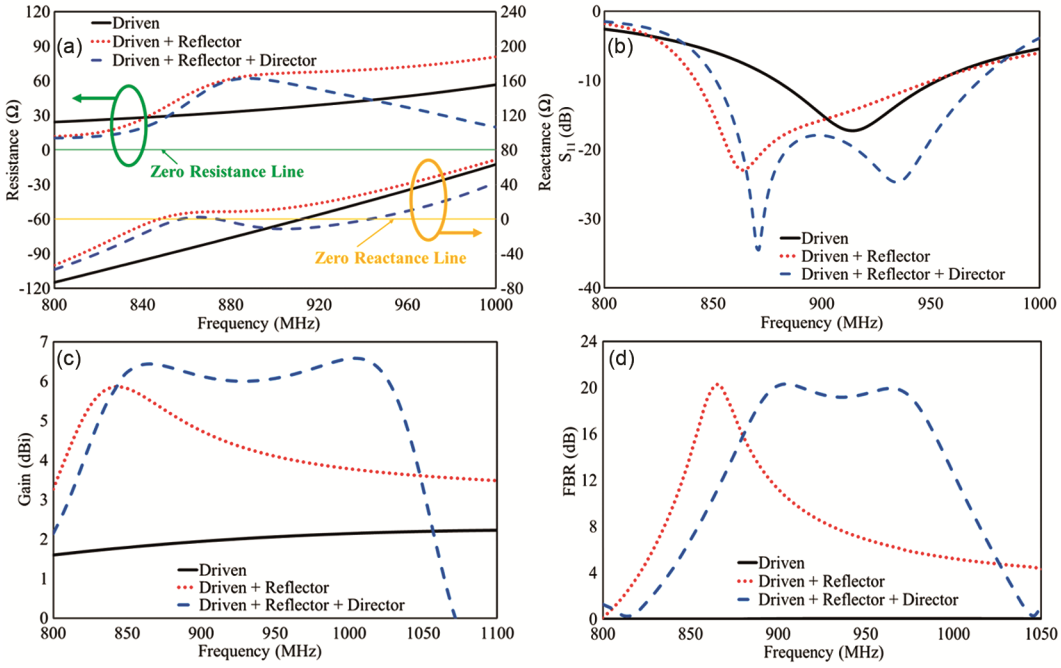

Fig. 3 — Analyses of design process of the proposed antenna. (a) Impedance (b) return losses (S11), (c) Gain, and (d) FBR

observed that below 910 MHz (i.e. when antenna length is less than λ/2) the reactance is negative depicting capacitive effect and for above 910 MHz (i.e. when antenna length greater than λ/2) it is positive representing inductive effect as shown in Fig. 3(a). This meandered driven element exhibits a -10 dB bandwidth of 74 MHz (879 – 953 MHz) with the gain of less than 2dBi and front to back ratio (FBR) is 0.5 dB as shown in Fig. 3(b) (c) and (d) respectively. For the improvement of performance parameters in the second stage of design (Antenna 2) a meandered reflector of length greater than λ/2 is designed on the same substrate in addition to the driven element as shown in Fig. 2(b). In order to avoid any impedance loading, the spacing (g2) between the radiating element and reflector element (Fig. 1) is required to be quarter wavelength[36]. In the proposed design to enhance the coupling between the driven element and reflector, the spacing 'g2' is optimized to be less than quarter wavelength (~0.186λ). The simulated responses are shown in Fig. 3. It is observed that by incorporating the reflector, -10 dB impedance bandwidth increases to 110 MHz (839 - 949) MHz as shown in Fig. 3(b). The zero reactance point shifted near 850 MHz as shown in Fig. 3(a). It is observed that the for the resonance frequency less than 850 MHz the antenna shows capacitive effect and after that it shows inductive effect. Further, in between the frequency range of reflector resonance (850 MHz) and driven element resonance (910 MHz), the resistance and reactance parts of impedance are near to 50 Ω and 0 Ω respectively as represented in Fig. 3(a).

This is clearly shows that capacitive effect of driven element below 910 MHz is nullified by the inductive effect of reflector above 850 MHz and makes the design to resonate resistively from 850-910MHz thereby enhances the impedance bandwidth to 110 MHz as shown in Fig. 3(b). The gain and FBR is 5.5 dBi and 20 dB respectively in lower UHF RFID ETSI band as shown in Fig. 3(c) and (d) respectively. The gain and FBR are 4 dBi and 6.5 dB respectively in the higher UHF RFID FCC band (Fig. 3(c) and (d)).It is observed from Fig. 3(a) that the reactance part of the impedance is significantly positive for FCC band which cause impedance mismatch thereby the reader antenna works poorly for this band. Moreover, the gain and FBR are also limited in the FCC band as represented in Fig. 3 (c) and (d). Therefore, in order to reduce the reactance in high RFID frequency region (FCC) a meandered parasitic element of length less than the driven element is placed in front of the driven element as shown in Fig. 2(c) (Antenna 3). In contrast to conventional Yagi-Uda structure the separation between the driven and parasite director element is chosen to be less than quarter wavelength (~0.073λ) to enhance the coupling between the driven element and meandered parasitic director element so that it radiate in higher frequency region as represented by S_{11} response shown in Fig. 3(b). It is noticed that the incorporation of director element creates zero reactance point at 943 MHz as shown in Fig. 3(a).This parasitic element shows capacitive effect below 943 MHz. This indicates that the capacitive effect of director element below 943 MHz is nullified by the inductive effect of combination of reflector and driven element above 910 MHz and makes the complete design consisting of three elements to resonate resistively from 850-972 MHz thereby enhances the impedance bandwidth to 122 MHz (850 MHz to 972MHz) as shown in Fig. 3(b). Further, the gain and FBR are also increased in higher frequency region (FCC band). The maximum gain and FBR of the designed reader antenna are 6.46 dBi and 19.75dB as shown in Fig. 3(c) and (d) respectively. The high front-to-back ratio (FBR) of the designed RFID antenna, ensures efficient radiation and minimizes the interference from unwanted directions. This improves the tag readability in real-time environments. To examine the contribution of individual elements of the designed antenna, the surface current distribution of the antenna is analyzed for low (ETSI) and high (FCC) frequency regions as shown in Fig. 4. As shown in Fig. 4(a), atlower frequency of the RFID band (866MHz), there isa high concentration of current at the reflector and driven element creating a constructive radiation in forward direction and increase the directivity of the antenna, indicating resonance within the lower frequency range as the reflector length is approximately half wavelength at 866 MHz. Moving to the middle frequency (910MHz), the current is mainly distributed at the driven element. Similarly, at the higher frequency (960MHz), the current distribution primarily favors the driven element and parasitic director element, as in higher frequency region director radiates in half wavelength mode. Additionally, referencing the gain responses depicted in Fig. 3 (c), it becomes apparent that the antenna

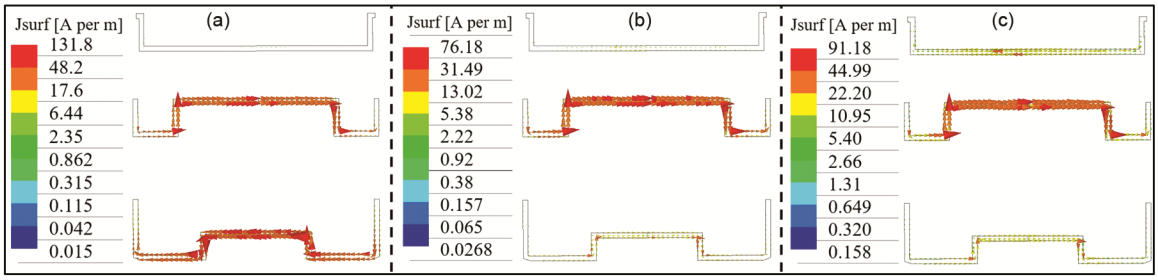

Fig. 4 — The simulated current distribution in antenna at (a) 860 MHz, (b) 910 MHz and (c) 960 MHz

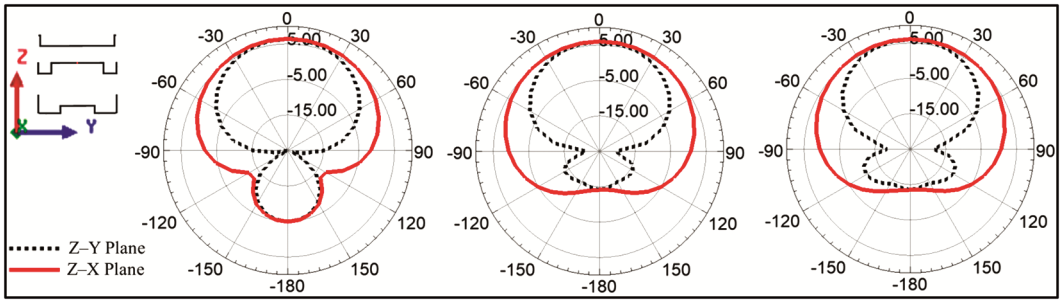

Fig. 5 — The simulated 2-D radiation pattern (a) 866 MHz, (b) 910 MHz, and (c) 953 MHz

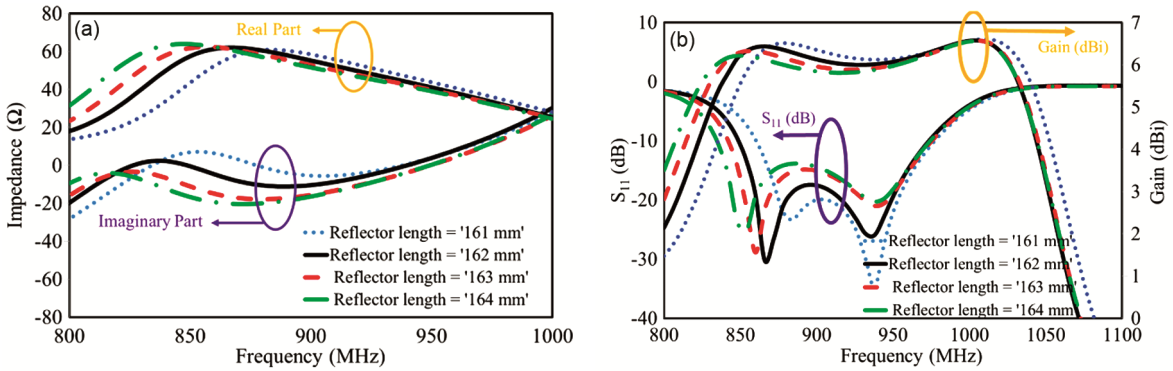

Fig. 6 — Effect of the variation of the reflector length on antenna parameters. (a) Impedance (b) return loss (S11) and gain

exhibits high gain in proximity to the resonant frequencies of both the director and the reflector and this indicate the antenna's wideband characteristics. The simulated far-field radiation patterns on the ZX and ZY-plane of the antenna for different frequency in UHF RFID band is shown in Fig. 5. It is observed that at three frequencies, the antenna represents the consistent directional radiation behavior in both the planes. The antenna's HPBW at regular intervals of UHF RFID band for ZX and ZY planes are listed in Table 2.

Table 2 — 3 dB Beamwidth in ZX and ZY-Plane at different frequencies

Frequency (MHz)	Z-X Plane	Z-Y Plane
866	125°	73 °
910	130 °	73 °
953	134 °	70.3°

2.2 Optimization of reflector and director lengths to achieve wide bandwidth

In order to get better physical insights of the designed antenna the effects of lengths of reflector and director is investigated. At first to optimize the length of the reflector, its length is varied from 162 mm to 164 mm. It is observed that as the reflector length increases the real part of the antenna impedance increases and imaginary part reduces with a left shift in their lower frequency portion as shown in Fig. 6(a). It is also noted that high frequency portion of the impedance and S_{11}remains unaltered as shown in Fig.6 (a) & (b).

This increases in the reflector length causes lower frequency resonating point of the antenna to shift leftwards thereby bandwidth increases as shown in Fig. 6(b). On the other hand this increase in bandwidth is achieved at the cost of small decrease in gain as shown in Fig. 6(b). Therefore, the optimal length of reflector is chosen as 162 mm.

Secondly, to optimize the length of the director, its length is varied from 116 mm to 142 mm. It is observed that as the length of the director element increases the real part of the antenna impedance decreases and imaginary part increases due to increase in inductive effect in their higher frequency portion as shown in Fig. 7(a). It is also noted that low frequency portion of the impedance and S_{11} remains unaltered as shown in Fig. 7(a) & (b). This increases in director length causes higher frequency resonating point of the antenna to shift leftwards thereby bandwidth decreases as shown in Fig. 7(b). On the other hand the reduction in bandwidth causes slight increase in gain as shown in Fig. 7(b). Therefore as a trade off in gain and bandwidth the optimal values of director length is chosen as 121mm.

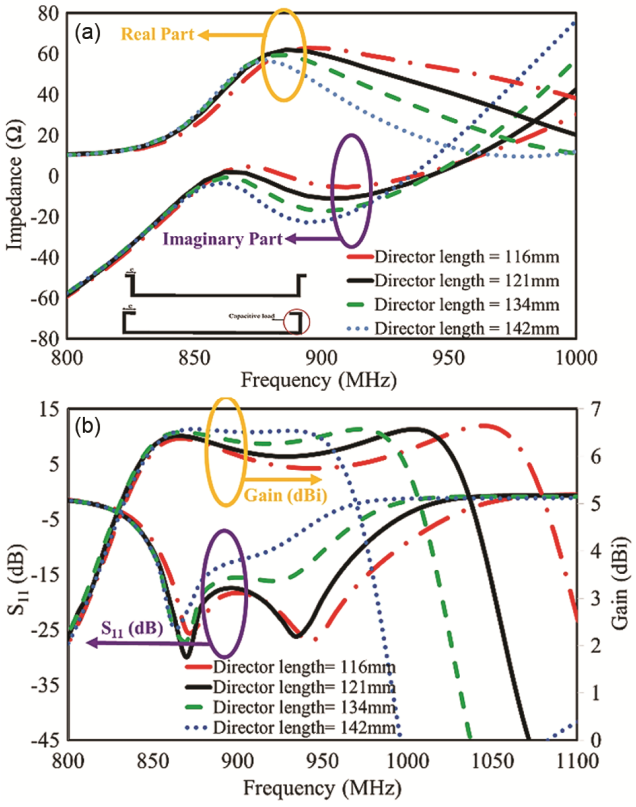

Fig. 7 — Effect of the variation of the reflector length on antenna parameters. (a) Impedance (b) return loss (S11) and gain

3 Experimental Measurements

A prototype of the RFID reader handheld antenna is fabricated on FR4 substrate of thickness 1.6 mm as shown in Fig. 8. The size of the fabricated tag is (100 × 100mm × 1.6) mm^3. To demonstrate the performance of the proposed antenna, the fabricated prototype is experimentally tested using the Skyetek Supernova RFID reader[37]. The reader power is set to 27 dBm for a single tag read testing scenario. The tag antenna reported in[38] having threshold power of -20.5 dBm is used to test the proposed reader antenna.

3.1 S_{11} Measurements

The 10 dB simulated and measured impedance bandwidth shown in Fig. 9 are 120 MHz (850-970MHz) and 125 MHz (845-970MHz) respectively, which are in close agreement with each other and cover the entire UHF RFID band (860-960MHz) regulated by ISO 18000-6C.

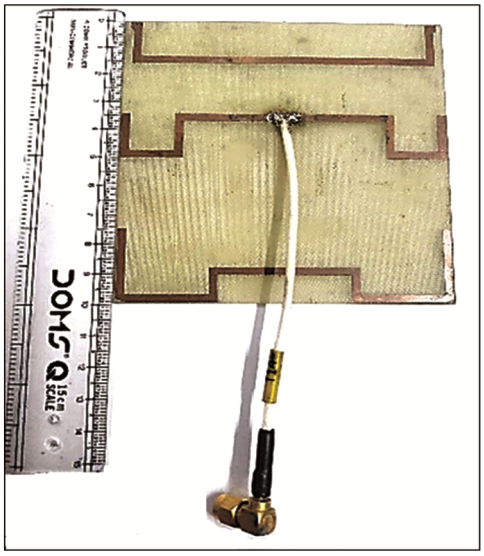

Fig. 8 — Fabricated prototype of RFID Reader Antenna

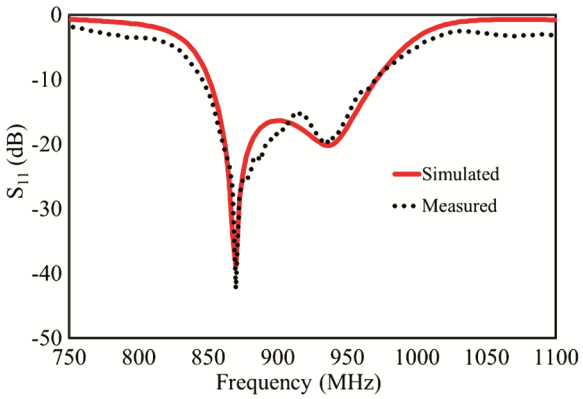

Fig. 9 — Simulated and measured S11 parameter of the prototype

3.2 Reading Range Measurements

The tag is placed at a different angled position in front of the reader module and the maximum reading range was measured, by keeping the tag in motion away from the reader to a point where it is maximally detectable for point–to-point transmission and reception. The reading range is measured for the two standard frequency bands that are ETSI (for the European countries and India, 866-869MHz) and FCC (for the US, 902-928MHz). Fig. 10 shows the measured reading range at different angles. It is observed that a symmetric unidirectional pattern is obtained and the maximum reading range obtained is greater than 15m in the ETSI band and greater than 10 m in the FCC band which agrees well with the theoretical prediction performed by using the Friis equation. The range of the tag not only depends on the EIRP (effective isotropic radiated power) of the reader antenna but also depends on tag chip threshold power which is -20.5 dBm in this case, tag antenna gain, polarisation, and tag antenna impedance matching with tag chip. As discussed in [38] the impedance matching of the tag antenna with the chip is not as good as in the FCC band as compared to the ETSI band, so due to this reason, the tag read range is reduced in the FCC band.

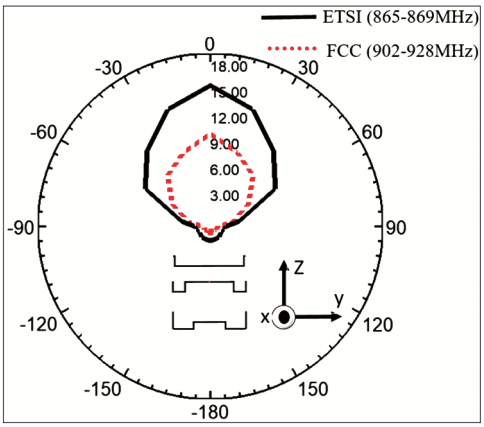

Fig. 10 — The measured reading range at different angle with respect to the reader module

The performance of the proposed tag antenna has been compared with the already reported RFID handheld antenna in terms of impedance bandwidth, gain, antenna size, radiation efficiency, and FBR in Table 3. As compared to the designed reader antennamost UHF RFID antennas, especially those designed for handheld applications discussed in[11-12,14,25] are larger in size. The proposed RFID reader antenna is thinner in comparison to the designs reported in[3-6,13,25,27] requiring more space for integration or resulting in a bulky, less user-friendly design. Therefore, the proposed compact antenna improves portability and user experience as compared to the many of the existing designs.Further, the proposed designed RFID reader antenna offers a

Table 3 — Various design approach with performance

Ref.	Bandwidth		Max Gain	Antenna Size	Size(λ)	Rad. Eff. (%)	FBR (dB)
[3]	910-925MHz	15	2.2 dBic	45mm×45mm×9mm	0.137×0.137×0.027	-	-
[4]	909-935MHz	26	4dBic	60mm×60mm×15mm	0.184×0.184×0.046	40	
[5]	810–960 MHz	150	4.5dBic	70mm×70mm×13.4mm	0.2×0.2×0.0395	70	
[6]	860-882MHz	22	4.5 dBi	86mm×86mm×12mm	0.249×0.249×0.0348	95	8.8
[7]	860-880MHz	20	1.9 dBic	Dia = 70mm, L= 8.6mm	0.203×0.024		
[10]	894–1030 MHz	136	2.91dBi	80mm×80mm×1.6mm	0.2565×0.2565×0.00513	-	-
[11]	710–1960 MHz	1250	3.4 dBi	116mm×116mm×1.6mm	0.516×0.516×0.00712	95	-
[12]	820-980MHz	160	5.7dBi	107mm×124mm×1.6mm	0.321×0.372×0.0048	80	17.2
[13]	830-910MHz	80	6dBi	> 100mm×100mm×6mm	> 0.29×0.29×0.0174	-	-
[15]	748-1076MHz	328	3.1 dBi	95mm×100mm×13.5mm	0.288×0.304×0.041	67	-
[17]	886-995MHz	109	5.42dBi	L = 91mm, dia =17.4mm	0.285×0.0545	-	-
[18]	865-915MHz	50	>6dBi	L= 130 mm, dia =85mm	0.385×0.2521	-	-
[19]	891-928MHz	37	5.5dBi	54mm×54mm×1.6mm	0.1637×0.1637×0.00485	-	-
[20]	877 - 987 MHz	110	1.4dBi	60mm×60mm×1.6mm	0.1864×0.1864×0.00497	-	-
[21]	815-925 MHz	110	5.5 dBic	83 mm×83 mm×1.6 mm	0.24×0.24×0.00464	89	-
[22]	931 – 960 MHz	73	Omni-dir	60mm×60mm×0.8mm	0.1899×0.1899×0.0025	-	-
[23]	913-931MHz	18	1.45dBi	40mm×50mm×1mm	0.1229×0.1536×0.0030	-	-
[24]	860-880MHz	20	6 dBi	120mm×65mm×6mm	0.348×0.1885×0.0174	80-85	8
[25]	840 - 960 MHz	120	2.5 dBi	105mm×105mm×1.9mm	0.315×0.315×0.0057	-	-
[26]	892-990MHz	98	3- 4.5dBi	90mm×90mm×1mm	0.2823×0.2823×0.0031	-	9-13
[27]	850-950MHz	100	4.8dBi	87mm×96mm×3.2mm	0.261×0.288×0.0096	89	10.2
This work	845-970MHz	125	6.46dBi	100mm×100mm×1.6mm	0.30×0.30×0.00484	>90	19.75

maximum gain of 6.46 dBi, which is higher than various handheld RFID antennas reported in[3-7,10–13,15,17-27] that typically provide gains around 2-5.5 dBi. Higher gain in an antenna leads to a stronger signal and more reliable communication, which is crucial for longer read ranges and robust performance in real-world applications. The 10 dB impedance bandwidth of the designed RFID reader spans 125 MHz (845-970 MHz), covering the entire UHF RFID band (860-960 MHz). Many existing RFID antennas discussed in[3-4,6,7,13,17-27] exhibits narrow impedance bandwidths thereby limits their uses for wideband operations. The designed RFID reader improves operational bandwidth, ensuring the antenna remains effective across the entire UHF RFID band.On the other hand, the proposed designed antenna achieves a FBR of 19.75 dB, which is notably high for a handheld RFID reader antenna. Higher FBR helps to reduce interference and ensures that the antenna's radiation pattern is focused towards the desired direction, improving the read range and reducing the likelihood of false reads. Many existing handheld antennas[6,12,24,26-27] reported low FBRs, resulting in lower efficiency or potential interference.The designed antenna demonstrates a radiation efficiency greater than 90%. High radiation efficiency ensures that a greater proportion of the power input to the antenna is radiated into free space, reducing losses and improving performance. Existing RFID antennas reported in[4-5, 12,15,21,24,27] exhibits low efficiencies between 40-85%. Therefore, the designed reader ante-nna offers a higher level of radiation effectiveness as compared to the many of the reported designs.The proposed antenna is designed using a meandered Yagi-Uda like structure, with carefully chosen dimensions for the reflector, director, and driven element, which help optimize impedance bandwidth and gain. The Yagi-Uda structure, known for its high directivity and efficiency, is well-suited for UHF RFID applications. While several of the existing RFID reader antennas discussed in [3-7,10-12,15-24] have not use such a meandered structured configurations. Hence this choice ensures a well-optimized balance between compactness, performance, and efficiency.

4 Conclusion

In this paper, a new wideband three element meandered Yagi-Uda reader antenna (driven element ≈ 0.45λ, reflector length ≈ 0.48λ, and director length ≈ 0.37λ) is designed and characterized. The antenna characteristics such as gain, radiation efficiency, FBR, radiation pattern, impedance bandwidth, and read range are discussed. The simulated and experimental results reveal that the proposed antenna provides an impedance bandwidth of 125MHz (845-970MHz), a high gain higher than 6 dBi, a high front-to-back ratio of 20dB, and a good total radiation efficiency of higher than 90% across the universal UHF RFID band. The effect of parasite meandered reflector and director on impedance bandwidth and gain bandwidth is also studied. Moreover, the antenna performance was evaluated with a UHF RFID reader in real-use cases where the read range of the tag was measured. The antenna is fabricated on an FR4 substrate and the overall size of the antenna is (100 × 100 × 1.6) mm^3. With this size, the proposed antenna is well suitable for RFID handheld reader applications.

References

1 Xavier F, Hikage O K, Pessoa M S de Paula & Fleury A L, *IEEE Proc Manag Global Economic Growth*, (2010) 1.

2 Chen Z N, Qing X & Chung H L, *IEEE Trans Microw Theory Technol*, 57 (2009) 1275.

3 Bang J H, Bat-Ochir C, Koh H S, Cha E J & Ahn B C, *IEEE Antennas Wirel Propag Lett*, 11 (2012) 1076.

4 Lin Y F, Lee C H, Pan S C & Chen H M, *IEEE Trans Antennas Propag*, 61 (2013) 5283.

5 Lin Y F, Chen H M, Chen C H & Lee C H, *Electron Lett*, 49 (2013) 442.

6 Hoang M H, Van Hoang T Q, Phan H P & Vuong T P, *IEEE Antennas Wirel Propag Lett*, 14 (2015) 1439.

7 Trinh L H, Lu K T, Nguyen M T, Truong N V & Ferrero F, *Prog Electromagn Res M*, 93 (2020) 43.

8 Boursianis A, Dimitriou A, Bletsas A & Sahalos J N, 2016 10th Eur Conf Antennas Propag (EuCAP), (2016) 1.

9 Gao B & Yuen M M F, *58th Electron Compon Technol Conf*, (2008) 1990.

10 Pan C Y, Su C C & Yang W L, *Frequenz*, 72 (2018) 181.

11 Ma R & Feng Q, *Prog Electromagn Res C*, 111 (2021) 97.

12 Hsu H T & Huang T J, *IEEE Trans Antennas Propag*, 61 (2013) 4852.

13 Nikitin P V & Rao K V S, *IEEE Antennas Propag Soc Int Symp*, (2010) 1.

14 Nikitin P, Rao K V S, Lam F S, Schatz S & Johnson J, *US Patent Appl*, (2009) 174.

15 Liu Q, Shen J, Liu H, Wu Y, Su M & Liu Y, *IEEE Antennas Wirel Propag Lett*, 14 (2015) 1326.

16 Chen H D, Tsai C H, Sim C Y D & Kuo C Y, *IEEE Antennas Wirel Propag Lett*, 12 (2013) 1460.

17 Zauind-Deen S H, Malhat H A & Awadalla K H, *28th Natl Radio Sci Conf (NRSC)*, (2011) 1.

18 Nikitin P V & Rao K V S, *IEEE Int Conf RFID*, (2010) 166.

19 Farswan A, Gautam A K, Kanaujia B K & Rambabu K, *IEEE Trans Antennas Propag*, 64 (2016) 771.

20 Lin Y F, Wang Y K, Chen H M & Yang Z Z, *IEEE Trans Antennas Propag*, 60 (2012) 1221.

21 Pakkathillam J K, Kanagasabai M & Alsath M G N, *IEEE Antennas Wirel Propag Lett*, 16 (2017) 149.

22 Chen W S & Huang Y C, *IEEE Antennas Propag Mag*, 55 (2013) 128.
23 Huang H Y, Wang B Z, Zang R, Liang M S, Wang Z & Tan M T, *IEEE Antennas Propag SocInt Symp (APSURSI)*, (2014) 1845.
24 Tatomirescu A, Alrabadi O & Pedersen G F, *IEEE Antennas Propag SocInt Symp (APSURSI)*, (2013) 1108.
25 El Mahgoub K, *ACES J*, 32 (2021) 1152.
26 Hua R C & Ma T G, *IEEE Trans Antennas Propag*, 55 (2007) 3742.
27 Kim S G, Song J J & Kim T W, *IEEE Int Wirel Symp (IWS*), (2014) 1.
28 Yadav R, Gotra S, Pandey V S & Singh B, Intelligent Computing and Communication Systems, Algorithms for Intelligent Systems, Springer, Singapore, (2021) 1845.
29 Yadav R, Verma A & Raghava N S, *Superlatt Microstruct*, 154 (2021) 106881.
30 Lim S & Iskander M F, *IEEE Antennas Wireless Propag Lett*, 8 (2009) 88.
31 Huang H C, Lu J C & Hsu P, *IEEE Trans Antennas Propag*, 63 (2015) 2342.
32 Xin Q, Zhang F, Sun B, Zou Y & Liu Q, Int Symp Antennas Propag EM Theory, Guangzhou, (2010) 289.
33 Yadav R, Pandey V S, Kumar S, et al., *J Opt Soc Am A*, 39 (2022) 1749.
34 Yadav R, Pandey V S & Kumar S, *J Mater Sci: Mater Electron*, 32 (2021) 1.
35 Yadav R, Pandey V S & Verma P, *Plasmonics*, (2024).
36 Kraus J D, Antennas, (McGraw-Hill, New York, NY, USA), 1988.
37 "UHF RFID reader Skyetek Supernova", Available: www.jadaktech.com.
38 Choudhary A, Sood D & Tripathi C C, *IEEE Antennas WirelPropagLett*, 17 (2018) 1755.